

Supporting Information for “Effectiveness of Global, Low-Degree Polynomial Transformations for GCxGC Data Alignment”

Davis W. Rempe,^{*} Stephen E. Reichenbach,^{*†} Qingping Tao,[†] Chiara Cordero,[‡] Wayne E. Rathbun,[§] Cláudia Alcaraz Zini[#]

^{*}University of Nebraska – Lincoln, Lincoln NE 68588-0115, USA

[†]GC Image, LLC, Lincoln NE 68505-7403, USA

[‡]Università degli Studi di Torino, I-10125 Torino, Italy

[§] Honeywell UOP, 25 E. Algonquin Rd. Des Plaines, IL 60017-5016, USA

[#]Universidade Federal do Rio Grande do Sul, 91501-970 Porto Alegre-RS, Brazil

ABSTRACT: This document provides supplemental information for “Effectiveness of Global, Low-Degree Polynomial Transformations for GCxGC Data Alignment”, submitted to *Analytical Chemistry*. Due to space constraints and for brevity of presentation, that paper presents results for only a few examples. This supplement provides additional results. For a general description of the samples, instrumentation, system settings, data preprocessing, alignment algorithms, and evaluation methodology, refer to the body of the paper.

Instrumentation for Diesel Sample Runs. For the analysis of the diesel sample, all run conditions were in accordance with UOP 990, with a modulation period of 8 s and sampling with a flame ionization detector (FID) at 200 Hz. Diesel sample runs used a LECO GCxGC FID system equipped with an Agilent 6890 GC and LECO GCxGC accessories (modulator and secondary oven).

Instrumentation for Wine Sample Runs. Wine samples (750 mL each) were protected from direct light and stored in a cool place. After opening the bottles, smaller volumes of each wine were placed in 200 mL screw-capped dark glass flasks and were frozen (-18°C) in order to avoid loss of volatiles until chromatographic analyses. Headspace microextraction (HS-SPME) was performed with one mL of wine, 0.3 g of sodium chloride at 55°C (\pm 0.9), and a DVB/CAR/PDMS fiber (Supelco, Bellefonte, PA) in 20 mL headspace screw-capped glass vials. SPME fibers were previously conditioned according to manufacturer’s instructions. The system employed for GC \times GC was an Agilent 6890N (Agilent Technologies, Palo Alto, CA) with a time-of-flight mass spectrometric detector (TOFMS) equipped with a CombiPAL autosampler (CTC Analytics, Zwingen, Switzerland), a secondary oven for the second chromatographic column, and a quadjet cryogenic modulator (two cold and two hot) where cold jets were supported by nitrogen gas cooled with liquid nitrogen. Desorption took place at 250°C, in the injection port, where the fiber was kept for five (5) minutes. Other parameters employed were: modulation period of 7 s, oven temperature offset of 10°C, transfer line temperature of 300°C, detector temperature 240°C, ionization energy of 70 eV, detector of voltage 1500 V, mass range 45 to 450 m/z, and data acquisition rate of 100 Hz. Carrier gas was helium (purity 5.0, White Martins, Pinhais, Brazil) and its linear velocity was 1.0 mL min⁻¹. Stationary phase of the first dimension column (¹D) was a DB-WAX (30 m \times 0.25 mm \times 0.25 μ m) and a DB-17ms (1.70 m \times 0.18 mm \times 0.18 μ m) in the second dimension (²D).

Instrumentation for Cocoa Sample Runs. For the analysis of the volatile fraction of cocoa samples, headspace solid-phase micro-extraction (HS-SPME) was performed on 1.00 g of cocoa nibs finely milled with liquid nitrogen at 45°C (\pm 0.9) for 40 minutes. A DVB/CAR/PDMS fiber (Supelco, Bellefonte, PA) was used in 20 mL headspace screw-capped glass vials. The GCx2GC-MS/FID runs with reverse-inject differential flow modulation used an Agilent 7890B GC unit coupled to an Agilent 5977A fast quadrupole MS detector (Agilent, Little Falls, DE) operating in EI mode at 70 eV, and a fast FID. The GC transfer line was set at 270°C. A scan range of 40-240 m/z with a scanning rate of 20,000 amu/s was used, and the spectra generation frequency was 35 Hz. The FID base temperature was 280°C, with H₂ flow of 40 mL/min, air flow of 240 mL/min, and make-up (N₂) of 450 mL/min, at a sampling frequency of 150 Hz. The system was equipped with reverse-inject differential flow consisting of one CFT plate connected to a three-way solenoid valve that receives a controlled supply of carrier gas (helium) from an auxiliary electronic pressure control module (EPC). Pulse time was set at 200 ms and modulation period of 3 s. The ¹D used a SolGel-Wax column (100% polyethylene glycol)(30 m \times 0.25 mm d_c , 0.25 μ m d_f) from SGE Analytical Science (Ringwood, Australia) coupled with a ²D OV1701 column (86% polydimethylsiloxane, 7% phenyl, 7% cyanopropyl) (5 m \times 0.25 mm d_c , 0.25 μ m d_f) from Mega (Legnano, Milan, Italy). Cocoa volatiles extracted by HS-SPME were thermally desorbed into the GC split/splitless injector port in split mode, with split ratio 1:20, and injector temperature 250°C. The carrier gas was helium at a constant flow of 0.3 mL/min in the ¹D and 20 mL/min in the ²D. The temperature program went from 50°C (0.5 min) to 250°C at 2°C/min (5 min). Connection between the ²D column and the two parallel detectors was by a three-way unpurged splitter (G3181B, Agilent, Little Falls, DE). The deactivated capillary to the MS detector was 0.17 m long with 0.1 mm d_c , and to the FID detector was 1.3 m long with 0.45 mm d_c . Split ratio was 25:75 (MS:FID).

The GCxGC-MS runs with thermal modulation used an Agilent 6890 unit coupled to an Agilent 5975C MS detector (Agilent, Little Falls, DE) operating in EI mode at 70eV. The GC transfer line was set at 270°C with scan range 40-240 m/z and a scanning rate of 12,500 amu/s. The spectra generation frequency was 29 Hz. The system was equipped with a two-stage KT 2004 loop-type thermal modulator (Zoex Corporation, Houston, TX) cooled with liquid nitrogen. The hot jet pulse time was set at 250 ms and used a modulation period of 3 s. The fused silica capillary loop dimensions were 1.0 x 0.1 mm (inner diameter). The ¹D used a SolGel-Wax column (100% polyethylene glycol)(30 m × 0.25 mm d_c , 0.25 μm d_f) from SGE Analytical Science (Ringwood, Australia) coupled with a ²D OV1701 column (86% polydimethylsiloxane, 7% phenyl, 7% cyanopropyl) (1 m × 0.1 mm d_c , 0.10 μm d_f) from Mega (Legnano, Milan, Italy). Cocoa volatiles extracted by HS-SPME were thermally desorbed into the GC split/splitless injector port in split mode, with split ratio 1:20, and injector temperature 250°C. The carrier gas was helium at a constant flow of 1.8 mL/min. Temperature program was from 40°C (1 min) to 200°C at 3°C/min and to 250°C at 10°C/min (5 min).

Additional Results for Time-Varied Data. Figure S1 shows the results for the alignment of two additional pairs of consecutive replicate diesel sample runs, along with additional training-set plots for the chromatogram pair presented in the paper. The misalignment between consecutive replicate runs indicates a benchmark for the lower bound of alignment performance due to systemic noise. Chromatogram pair 18 and 19 were discussed in the paper. For consecutive replicate diesel sample runs 17 and 18, the ¹D misalignment is about 0.0176 min, and the ²D is about 0.0156 s. For replicate runs 19 and 20 the ¹D misalignment averages 0.0177 min, and the ²D is about 0.0089 s. These ¹D values are less than the modulator sampling noise level for the diesel sample chromatograms (calculated in the paper). The ²D misalignments are in line with the benchmark used in the paper.

Figure S4 shows the performance of the global and local algorithms for the alignment of all six pairings of diesel sample chromatograms acquired over various periods of time. (Testing-set figures for pairing 012011 and 061413 are presented in the paper.) In each test, every method offers significant improvements in alignment for both chromatographic dimensions. In the ¹D, the initial misalignment of the chromatogram pairs ranges from about 0.07 min to over 0.83 min, many times greater than the benchmark. The third-degree polynomial tends to reach around 0.06 min whereas the affine and second-degree polynomial reach just under 0.07 min. The local algorithm averages just under 0.08 min.

In the ²D, the initial misalignment ranges from 0.06 s to about 0.44 s. The third-degree polynomial reaches the lowest RMSE in all but one of the results from Figure S4, averaging about 0.02 s. The second-degree polynomial is about the same. The affine and local methods still improve the initial misalignment, but only get to about 0.03 and 0.04 s, respectively. These results are consistent with those presented in the paper.

Additional Results for Sample-Varied Data. Figure S2 shows the results for alignment of two additional pairs of consecutive replicate wine sample runs, along with additional training-set figures for the pair presented in the paper. The 2011 pair is discussed in the paper. For the ¹D, the benchmarks from both additional pairs are less than the modulation sampling noise level of 0.034 min, like the one presented in the paper. In the ²D, the benchmark for both pairs is just over 0.015 s, right around the benchmark used in the paper of 0.01725 s.

Figure S5 shows the cross-validation performance of the alignment methods for all three pairs of chromatograms from different wine samples run in a very short period of time. The 2011, 2012 pair is discussed in the paper. In the ¹D, the initial misalignments are just barely greater than the benchmark RMSE. Because of this, no method is able to improve on the initial misalignment in either test. The initial misalignment between pairs in the ²D is around 0.02 s, also just above the benchmark value. So, there is little improvement on the alignment from any method. These results are in line with those found in the paper.

Table S1 summarizes the results of all three cross-validation experiments run on the wine chromatograms. It shows the minimum testing set RMSE reached for all alignment methods in both dimensions along with the average initial misalignment. The cells marked red are RMSE values greater than the average initial misalignment for that experiment.

Figure S6 visualizes the wine alignment results by plotting the minimum RMSE reached by each method against the average initial misalignment. The red dot-dashed line shows the RMSE benchmarks. The black dashed line shows the identity function – where the initial misalignment and minimum RMSE would be equal. A point above this line indicates that a method's resulting alignment is worse than it initially was, and one below offers an improvement. Each alignment method is represented by a different colored point. Between the two dimensions, several points from the third-degree polynomial and local method slightly worsen the initial misalignment (as shown in data points above the dashed line). When the points fall under the identity function, it is not by much, showing negligible improvement on the wine chromatogram alignment. These data support the idea that if two chromatograms have only a small initial misalignment, it may be better not to perform any alignment operation at all.

Additional Results for Instrument-Varied Data. Figure S3 shows the results for the alignment of two additional pairs of consecutive replicate cocoa sample runs, along with additional training-set figures for the pair presented in the paper. The top row aligns replicate sample runs performed on a flow modulation platform, and the bottom two rows were performed on a thermal modulation platform. The Thermal 2, 3 pair is discussed in the paper. For the other pairs in the ¹D, the benchmarks are about 0.037 min and 0.043 min, respectively. These are consistent with the 0.0412 min benchmark used in the paper. For the ²D, the average initial misalignment are about 0.03 s and 0.022 s, respectively, right around the paper benchmark of

0.0257 s. All methods did improve the alignment of the replicate flow-modulated chromatograms, indicating that there was a systematic misalignment between them. This is due to a small phase-roll affected by the alignment algorithms.

Figure S7 shows the cross-validation performance of the alignment methods on all six pairs of chromatograms acquired on different modulation platforms. The Flow 2, Thermal 1 pair is discussed in the paper, but additional training set plots are presented here. All methods significantly improved alignment in both dimensions. In the ¹D, the initial misalignments are consistently around 23.2 min, well above the benchmark. Across these six experiments, the affine transformation is able to reach about 0.48 min, the local algorithm from Gros et al. is about 0.51 min, and the second and third-degree polynomials reach about 0.53 min. As observed in the paper, the higher-degree polynomials might require more peak-pairs for maximal performance.

In the ²D, the initial misalignment is around 0.5 s. The second-degree polynomial reaches a minimum RMSE of about 0.031 s on average, the third-degree polynomial and local algorithm are both around 0.038 s, and the affine transformation averages around 0.046 s. These values are consistent with the example presented in the paper. All are effective, achieving between about 96% and 99% improvement.

Maximum Alignment Error. All figures presented so far have shown the root-mean-square-error (RMSE) with respect to retention times of matched peaks in a chromatogram pair. This metric indicates average-case performance of an alignment method, but the worst-case scenario must also be considered. Figures S8, S9, and S10 show the average maximum absolute alignment error (MAE) across all trials run for each training set size. The standard deviation of this MAE is also shown. Figure S8 is for the diesel runs, Figure S9 is for the wine runs, and Figure S10 is for the cocoa runs.

Across all experiments, behavior in both chromatographic dimensions is similar. If the training set has enough peak pairs, all methods reach a similar MAE for the testing set. The number of peak-pairs required to reach this convergent value differs between the different alignment methods. The local method from Gros et al. and the affine transformation require a much smaller training set than the second and third-degree polynomials in order to reach a lower MAE. This is consistent with the corresponding RMSE behavior. For the diesel runs in the ²D, the local algorithm tends to have a higher standard deviation than the other methods, but this trend does not hold in the wine and cocoa experiments.

Sample Chromatograms. Figures S11 through S14 show examples of the sample chromatograms and peaks used for alignment experiments. Figure S11 shows a diesel sample chromatogram acquired on June 14, 2013. All diesel chromatograms, including the replicate runs, look very similar to this one. The yellow circles show the 112 peaks that correspond across all diesel chromatograms and were used as alignment points.

Figure S12 shows a wine sample chromatogram acquired from the second run of the 2011 vintage sample. Because

misalignment is so minimal between wine chromatograms, they all look nearly identical to Figure S12. The yellow circles show the 78 peaks used for alignment of the wine chromatograms.

Figures S13 and S14 show a cocoa sample chromatogram acquired on a system using a thermal and flow modulator, respectively. The two other thermal modulated chromatograms used in experiments look very similar to S13, and the one other flow modulator chromatogram resembles Figure S14. The yellow circles show the 33 peaks used for alignment of cocoa sample chromatogram pairs.

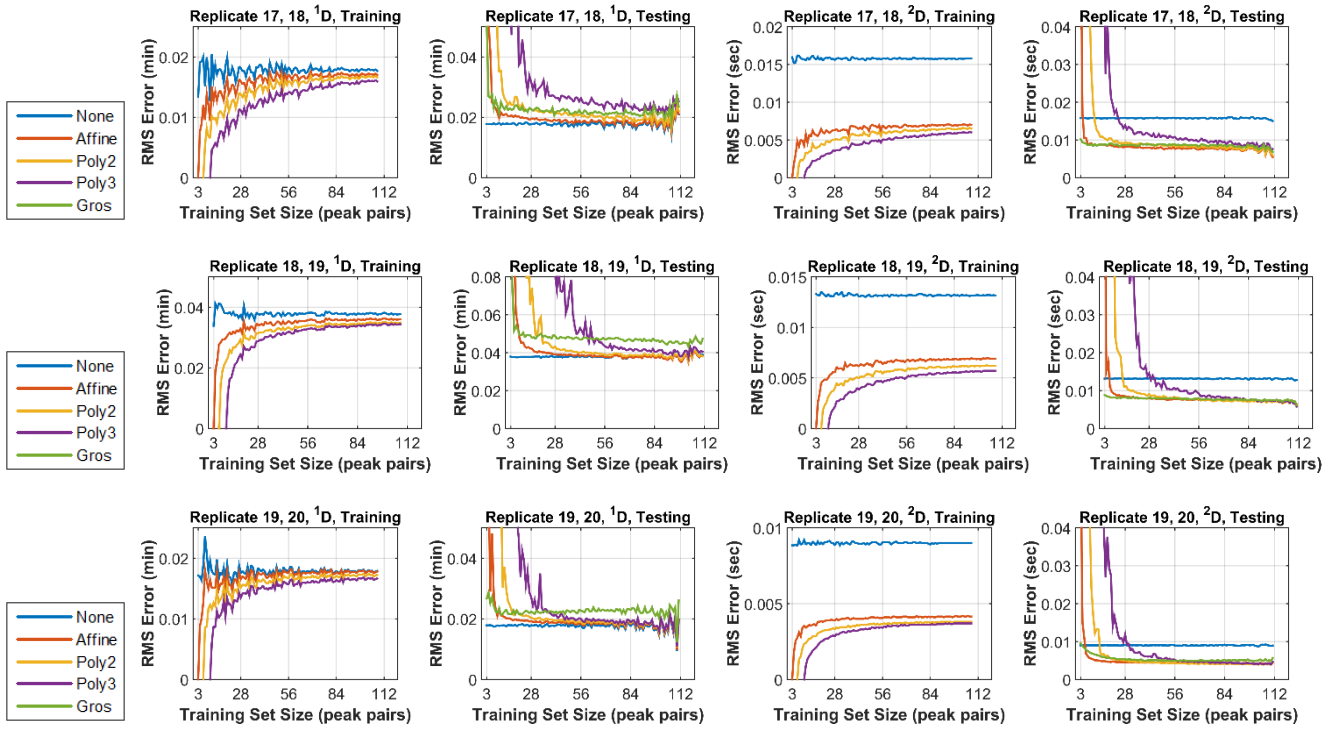


Figure S1. Cross-validation retention-time RMSE results as a function of training set size for consecutive replicate runs of a diesel sample. From left to right, the RMSE is shown for the ^1D with the training set, ^1D with the testing set, ^2D with the training set, and ^2D with the testing set. The performance of the local algorithm from Gros et al. is only shown in the testing plots because it is guaranteed to perfectly align the training set. The top row is for chromatograms from diesel runs #17 and #18, the middle row is for runs #18 and #19, and the bottom row is for runs #19 and #20.

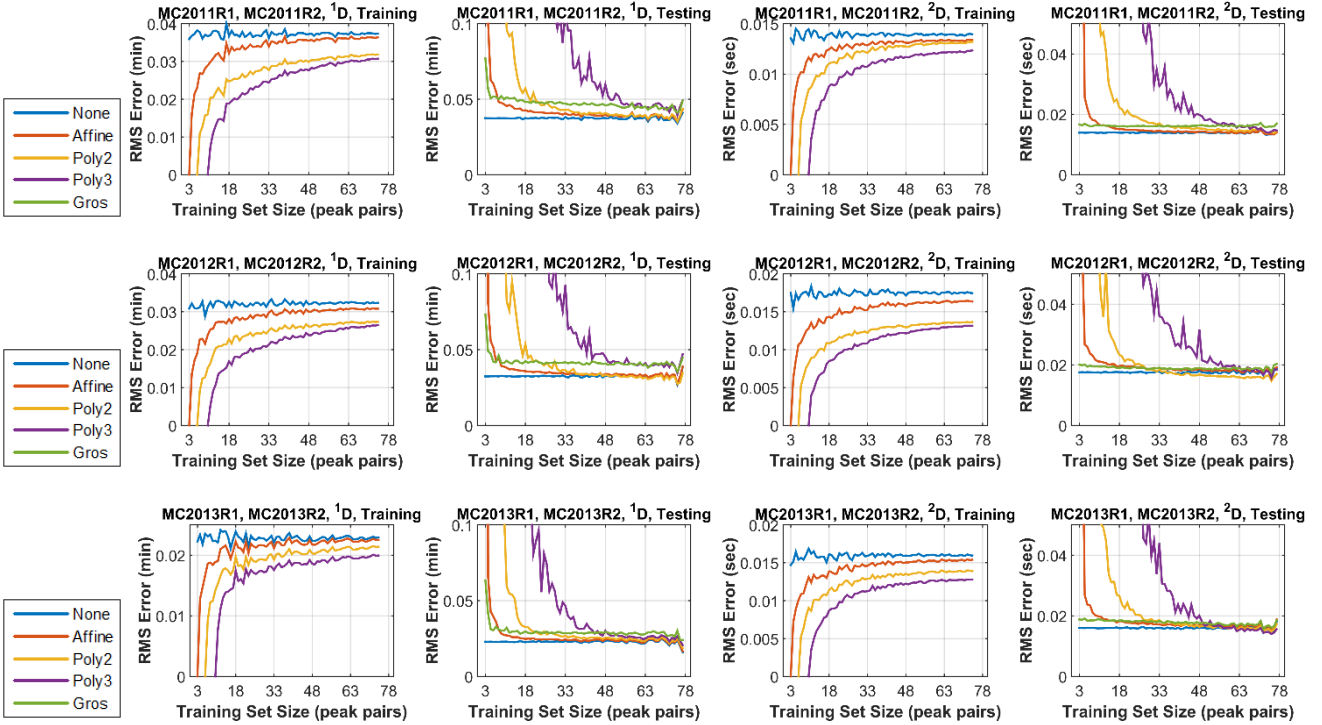


Figure S2. Cross-validation retention-time RMSE results as a function of training set size for consecutive replicate runs of the various wine samples. The names correspond to the vintage year of the wine sample. The top row is for chromatograms from vintage year 2011, runs #1 and #2. The middle row is for chromatograms from vintage year 2012, runs #1 and #2. The bottom row is for chromatograms from vintage year 2013, runs #1 and #2.

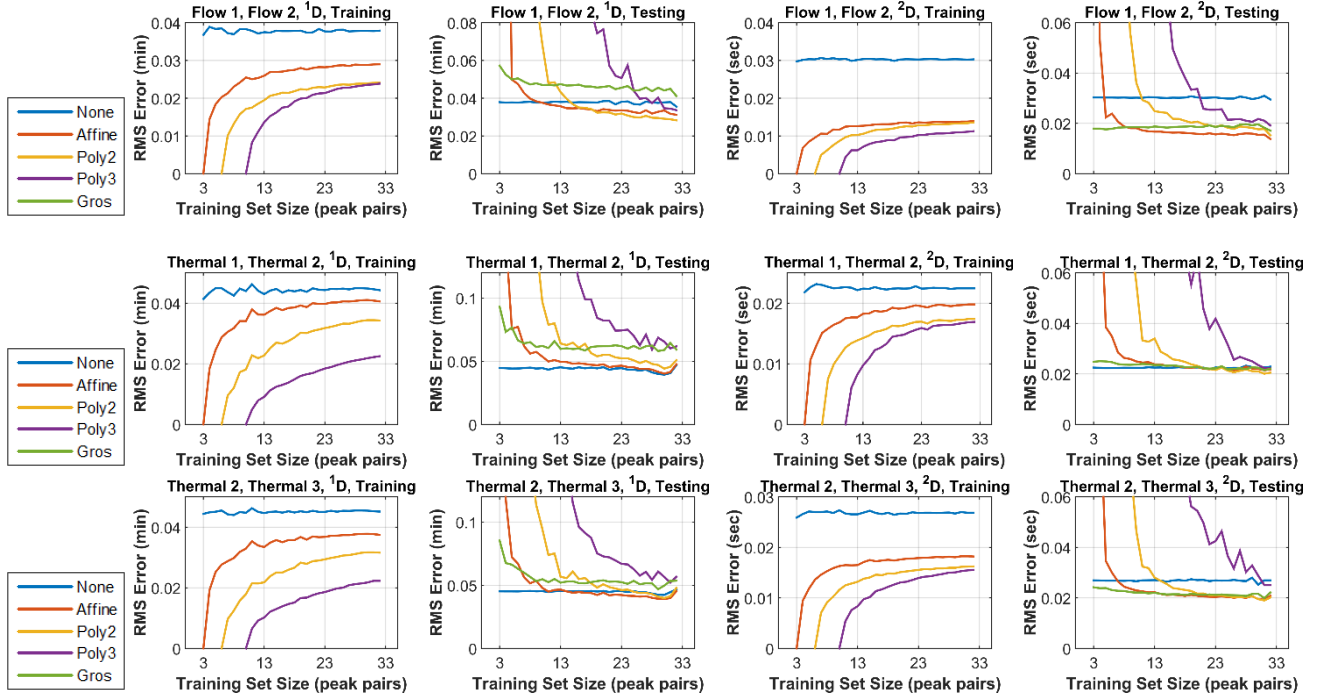


Figure S3. Cross-validation retention-time RMSE results as a function of training set size for consecutive replicate runs of a cocoa sample using different modulation platforms. The top row is for chromatograms from runs #1 and #2 using a flow modulator. The middle row is for chromatograms from runs #1 and #2 using a thermal modulator. The bottom row is for chromatograms from runs #2 and #3 using a thermal modulator.

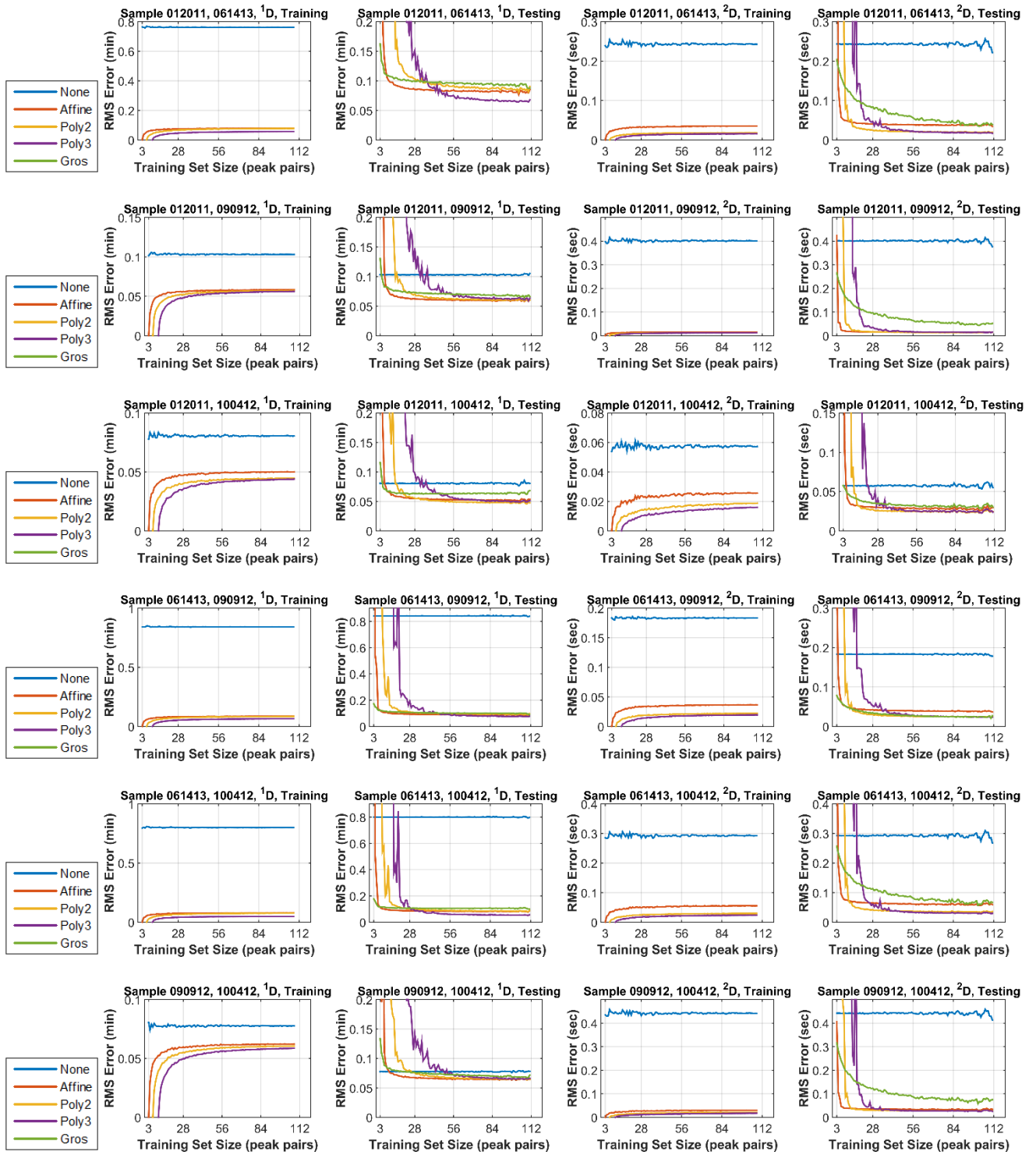


Figure S4. Cross-validation retention-time RMSE results as a function of training set size for chromatograms produced from the same diesel sample. From left to right, the RMSE is shown for the ^1D with the training set, ^1D with the testing set, ^2D with the training set, and ^2D with the testing set. The names of the samples correspond to the acquisition date (i.e. for the top row January 20, 2011 and September 9, 2012). Each row is for a different chromatogram pair.

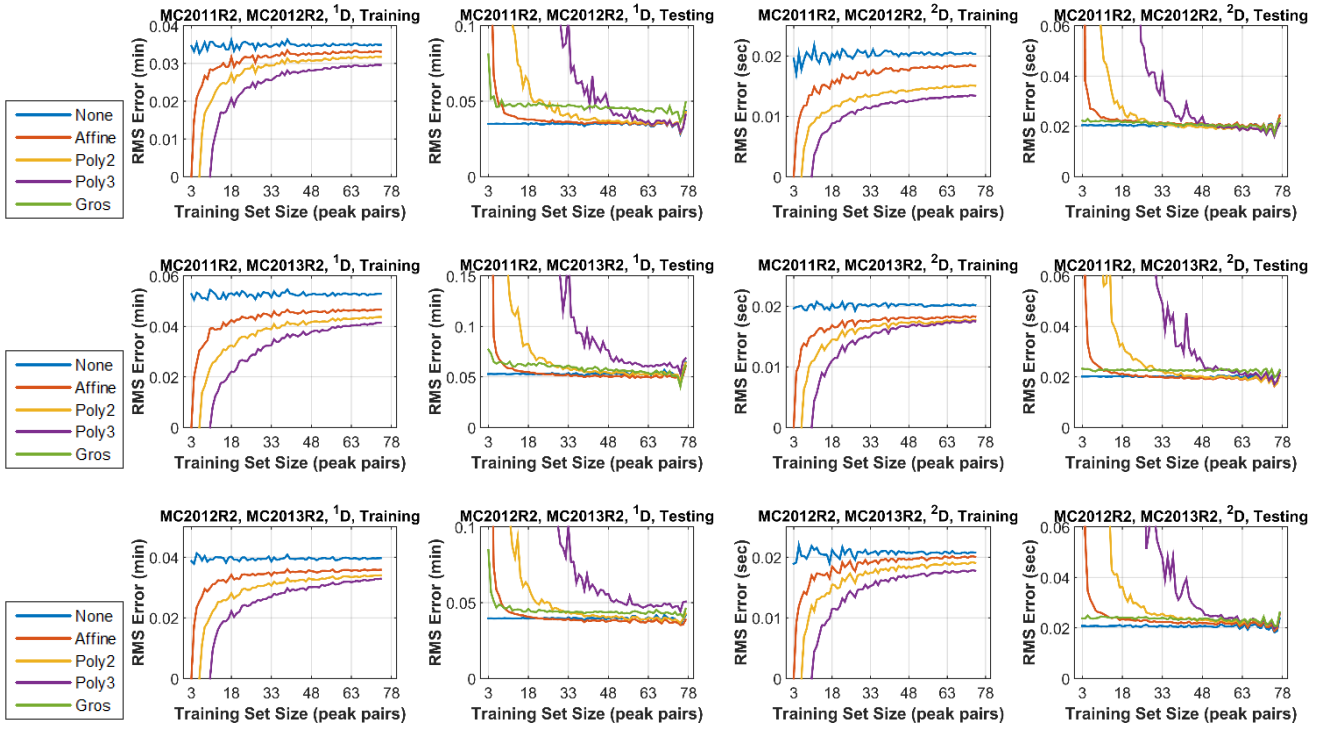


Figure S5. Cross-validation retention-time RMSE results as a function of training set size for alignment of two different wine sample chromatograms. The names correspond to the vintage year of the wine sample. For example, the top row is for chromatograms from the second runs of the 2011 and 2013 samples.

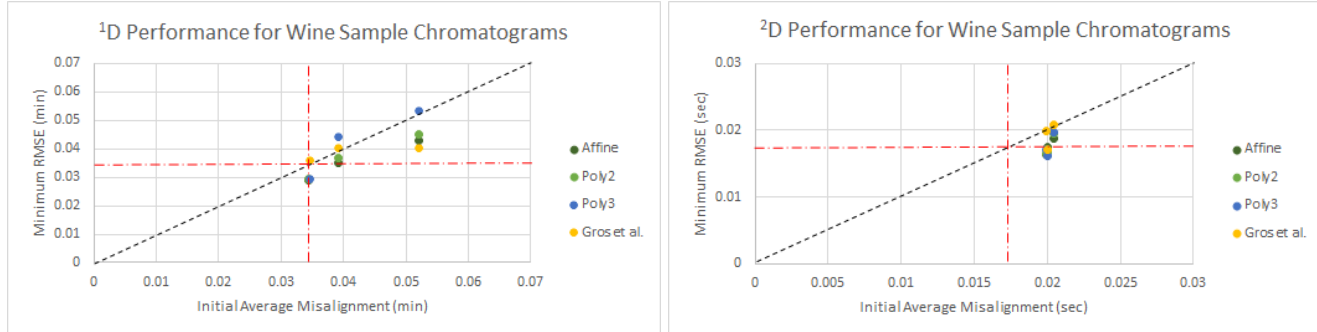


Figure S6. Minimum testing-set RMSE reached by the alignment methods on the wine sample chromatograms relative to the average initial misalignment. The red dot-dashed line shows the benchmark RMSE values (0.034 min and 0.01725 sec). The black dashed line shows the identity function – where the initial misalignment and minimum RMSE would be equal. A point above this line indicates that a method's resulting alignment is worse than it initially was, and one below offers an improvement.

Chromatograms	Minimum RMSE Reached by Alignment Methods in the ¹ D (min) and ² D (sec) for Wine Chromatograms									
	None (Avg.)		Affine		Poly2		Poly3		Gros et al.	
	¹ D	² D	¹ D	² D	¹ D	² D	¹ D	² D	¹ D	² D
2011-2012	0.0344	0.0200	0.0289	0.0175	0.0294	0.0167	0.0297	0.0161	0.0362	0.0171
2011-2013	0.0520	0.0199	0.0427	0.0164	0.0452	0.0166	0.0533	0.0171	0.0406	0.0198
2012-2013	0.0391	0.0204	0.0352	0.0188	0.0367	0.0195	0.0442	0.0197	0.0405	0.0208
Average	0.0418	0.0201	0.0356	0.0176	0.0371	0.0176	0.0424	0.0176	0.0391	0.0192

Table S1. Minimum testing-set RMSE reached by each alignment method in both the first and second chromatographic dimensions for all three experiments run with the non-replicate chromatograms from the wine samples. The “None” columns are the average initial misalignments, not the minimum. The red boxes indicate where the initial misalignment was made worse by a method. On average, no method was able to improve upon the initial alignment significantly in either dimension.

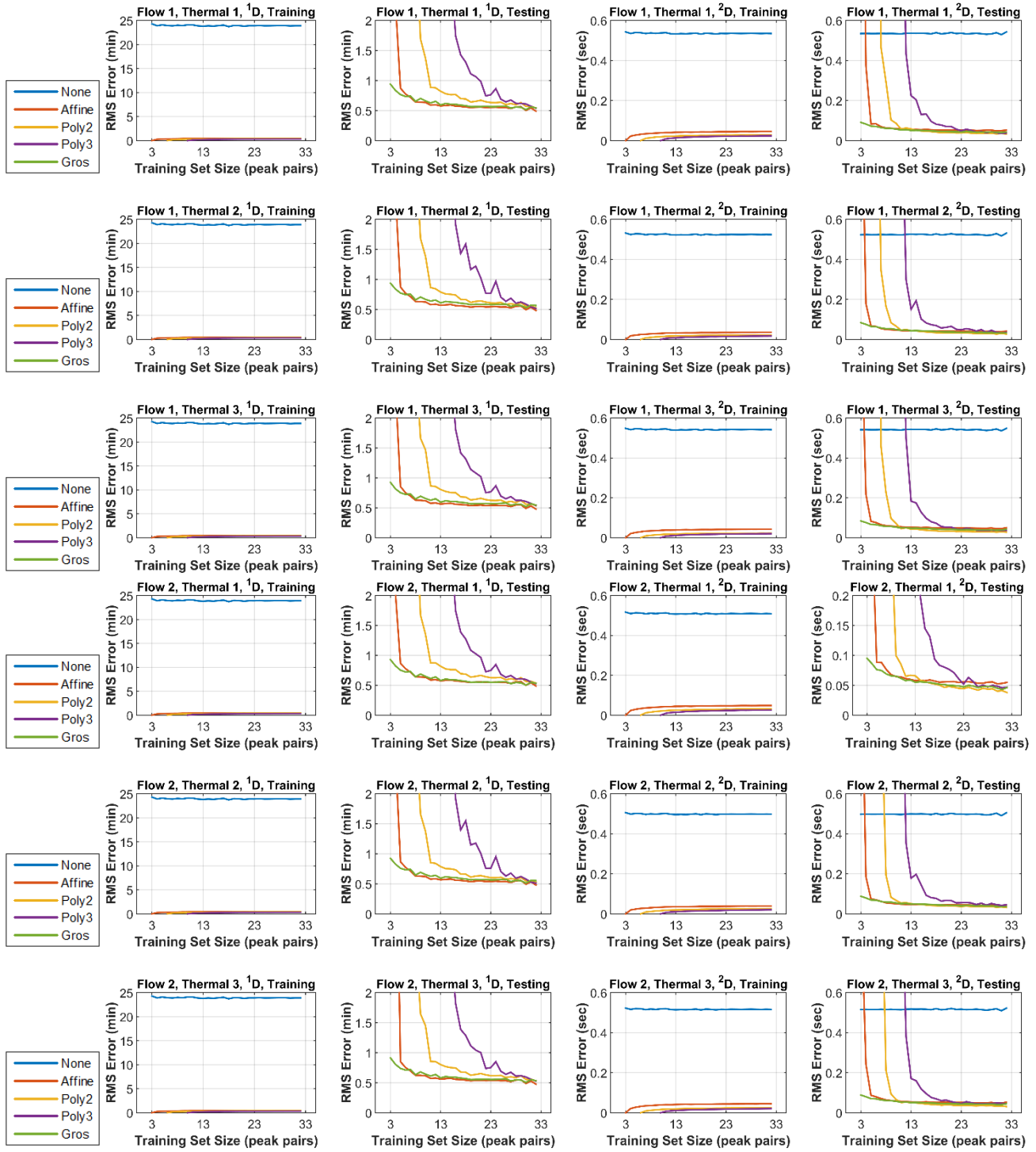
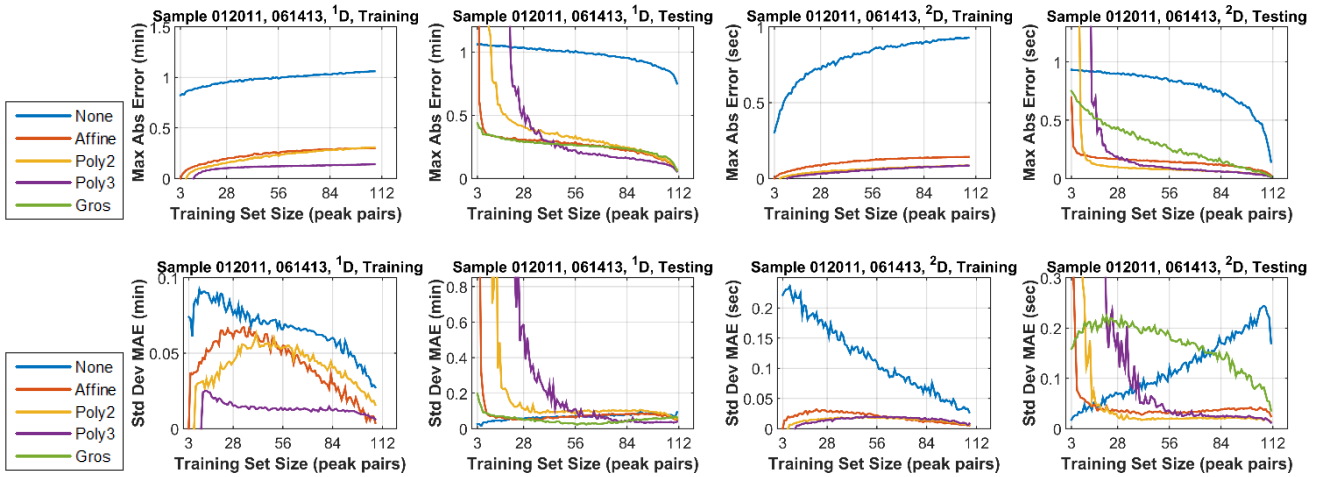
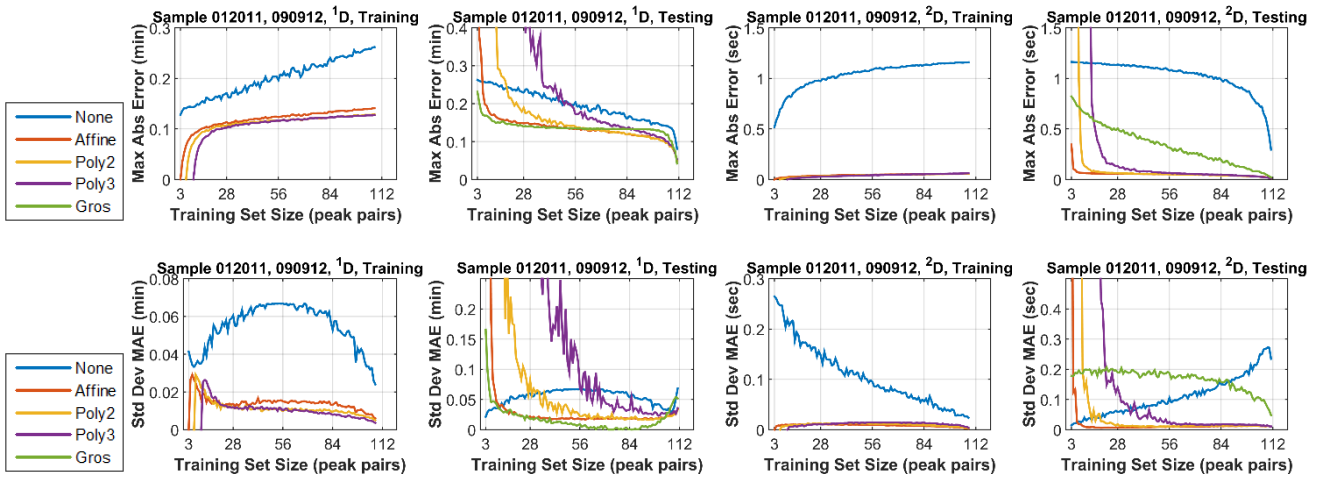


Figure S7. Cross-validation retention-time RMSE results as a function of training set size for chromatograms produced from the same cocoa sample but using two different modulation platforms. Each row is a pair of chromatograms from two different runs. For example the top row is for chromatograms from run #1 on the flow modulator, and run #1 on the thermal modulator.

A. Runs 012011 and 061413.



B. Runs 012011 and 090912.



C. Runs 012011 and 100412

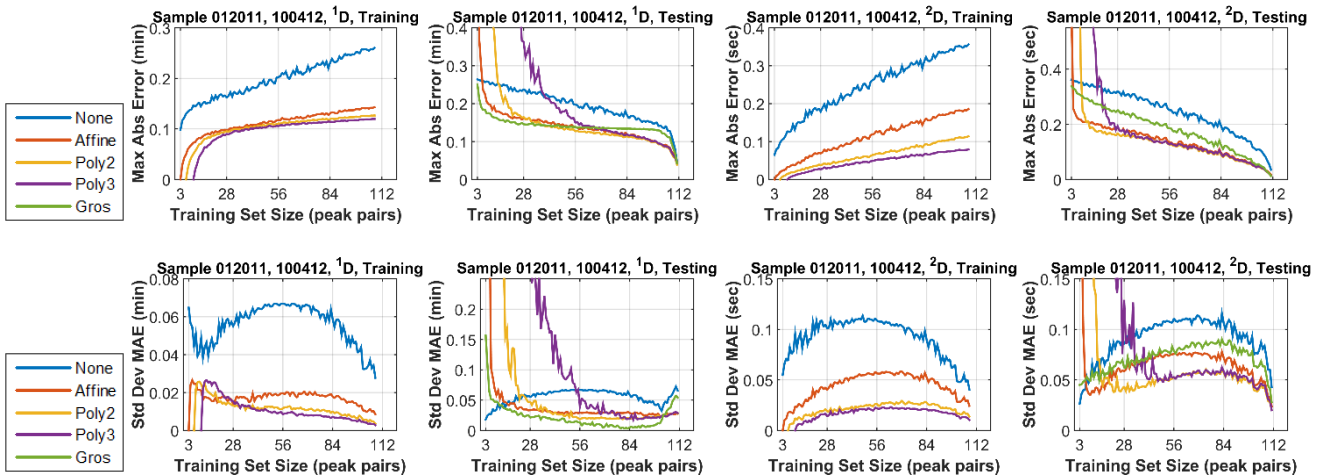
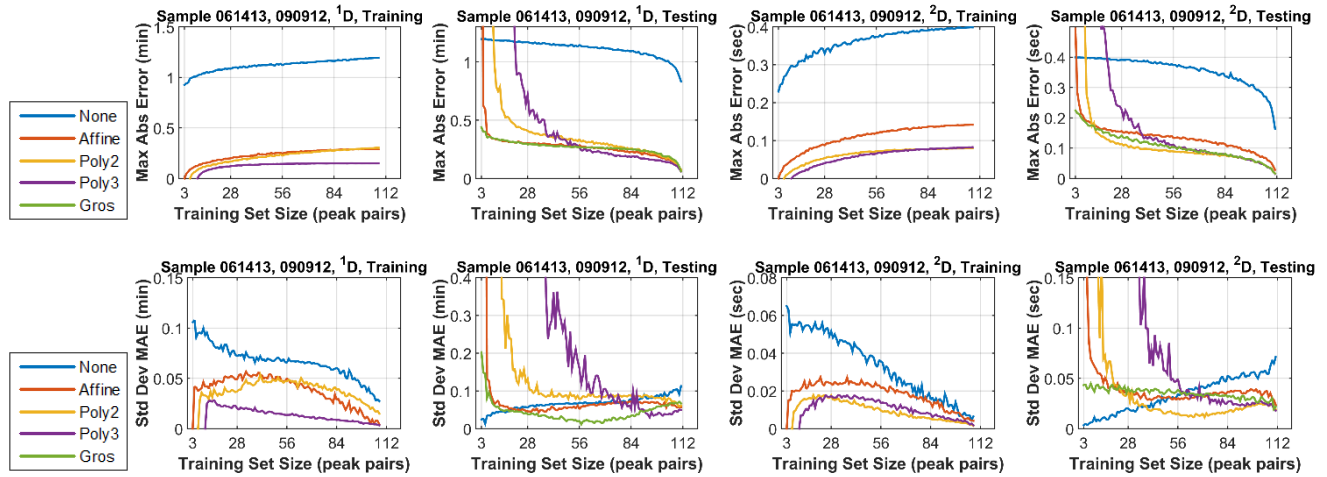
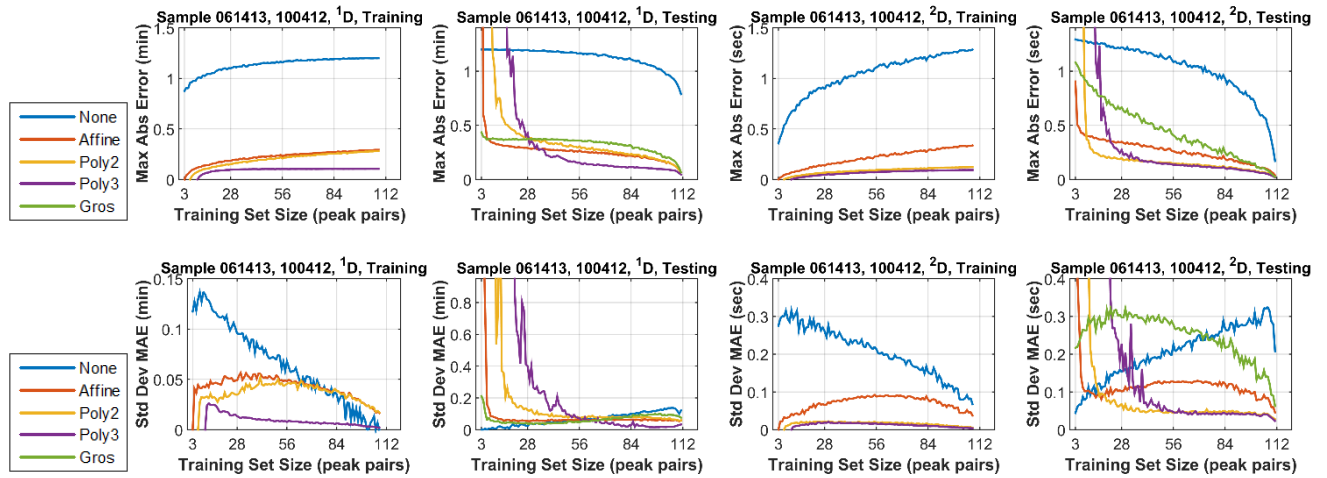


Figure S8. Maximum absolute error as a function of the training set size for alignment of GCxGC diesel sample chromatograms. Columns from left to right are for ¹D with the training set, for ¹D with the testing set, for ²D with the training set, and for ²D with the testing set. Sets of rows with maximum absolute error on the top row of each set and the standard deviation of maximum absolute error on the bottom row of each set are for: A. Runs 012011 and 061413, B. Runs 012011 and 090912, C. Runs 012011 and 100412, D. Runs 061413 and 090912, E. Runs 061413 and 100412, and F. Runs 090912 and 100412.

D. Runs 061413 and 090912.



E. Runs 061413 and 100412.



F. Runs 090912 and 100412.

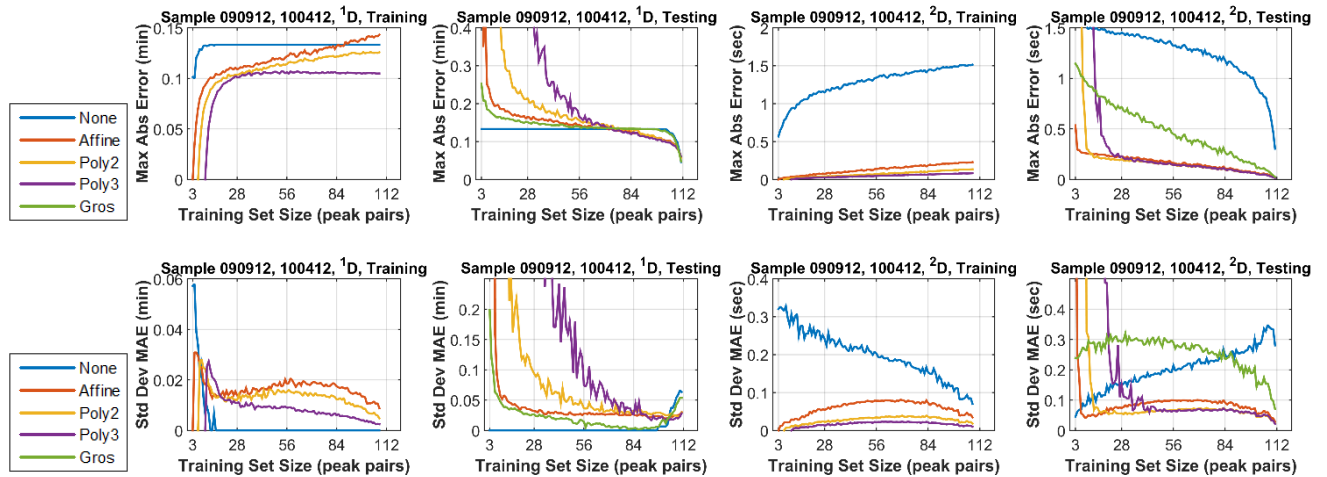
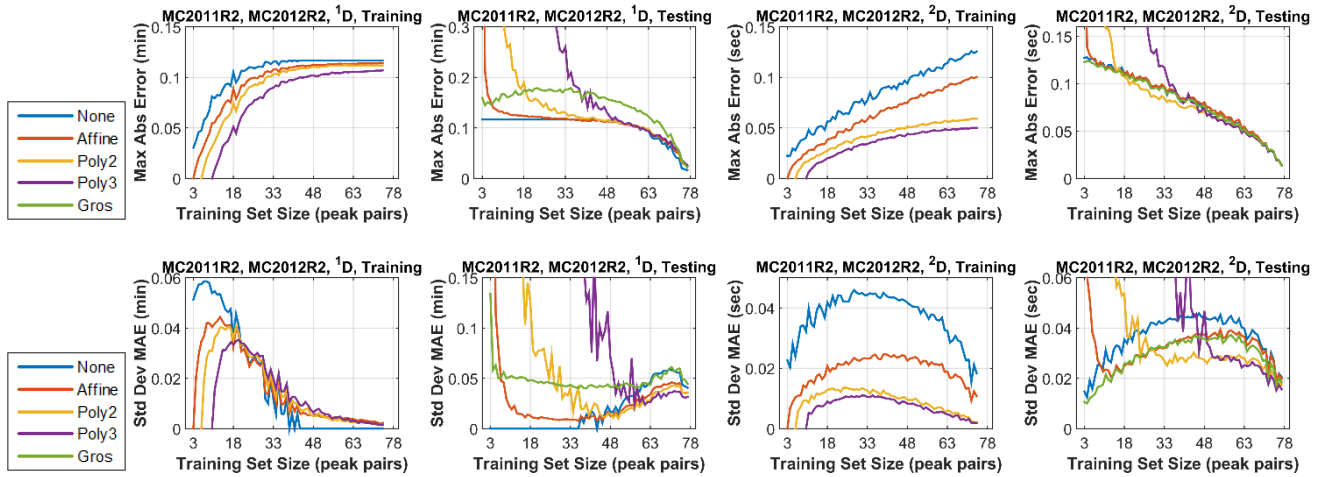
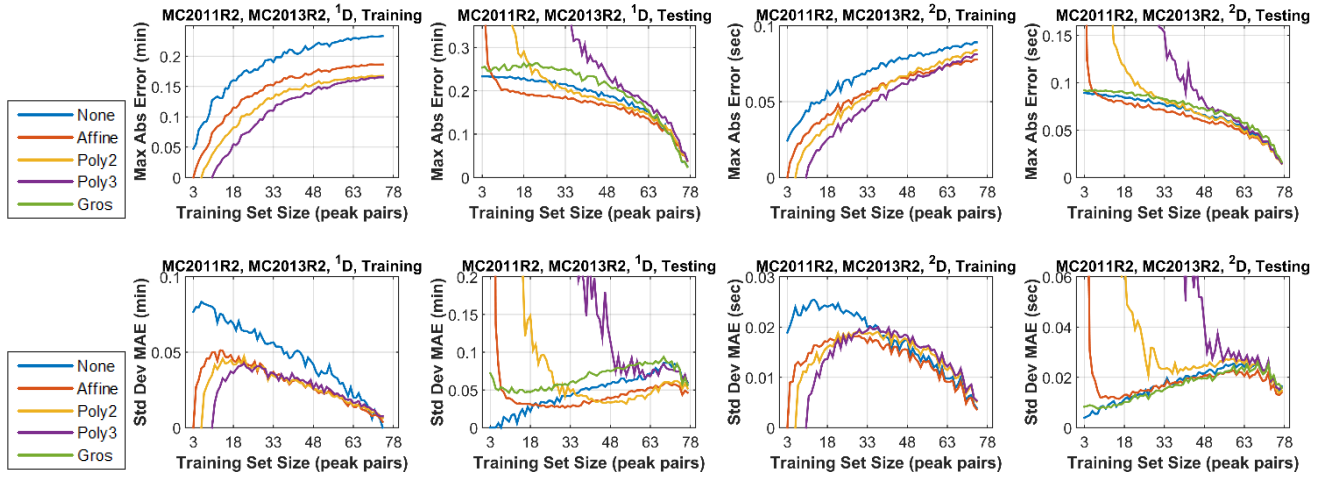


Figure S8 continued.

A. Samples 2011, 2012, Runs #2.



B. Samples 2011, 2013, Runs #2.



C. Samples 2012, 2013, Runs #2.

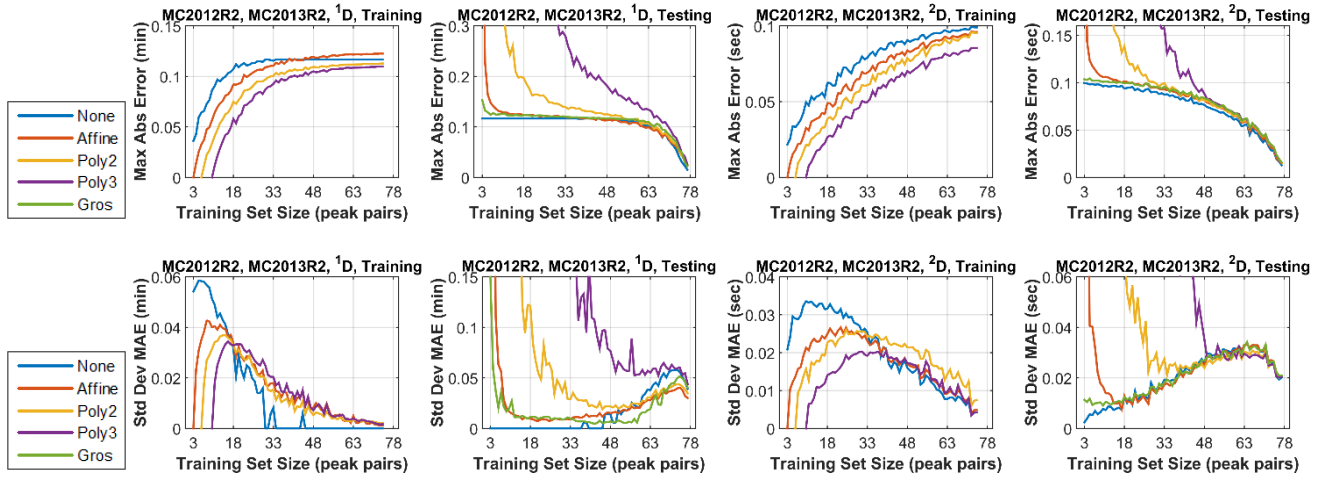
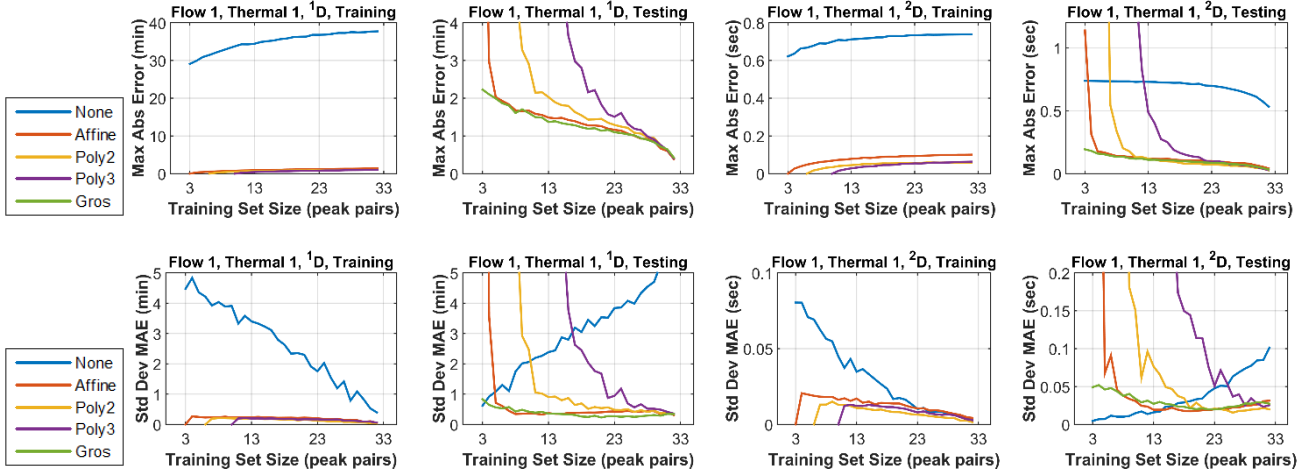
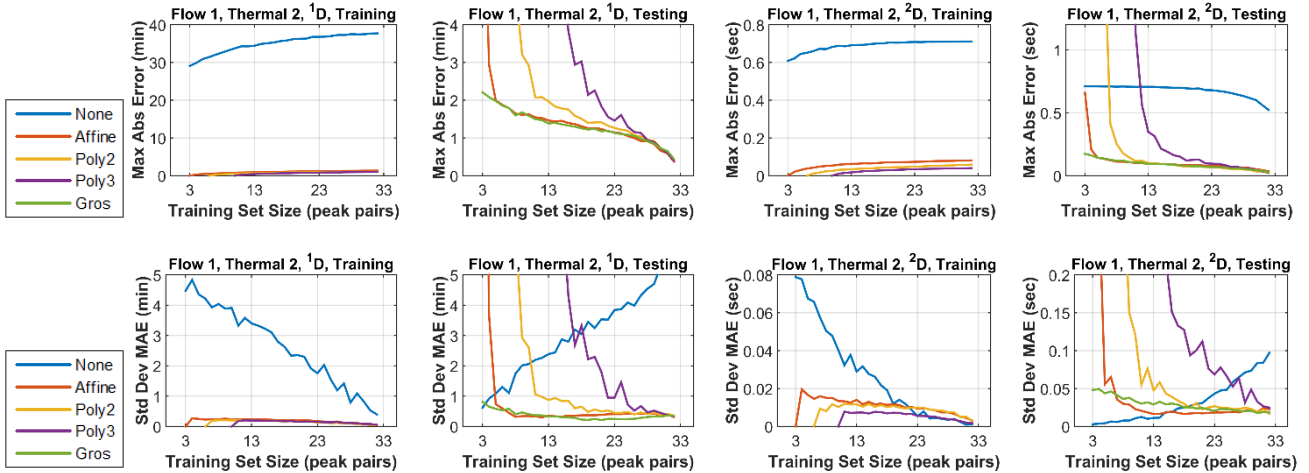


Figure S9. Maximum absolute error as a function of the training set size for alignment of GCxGC wine sample. Columns from left to right are for ^1D with the training set, for ^1D with the testing set, for ^2D with the training set, and for ^2D with the testing set. Sets of rows with maximum absolute error on the top row of each set and the standard deviation of maximum absolute error on the bottom row of each set are for: A. Samples 2011, 2012, Runs #2, B. Samples 2011, 2012, Runs #2, and C. Samples 2012, 2013, Runs #2.

A. Runs #1 and #1.



B. Runs #1 and #2.



C. Runs #1 and #3.

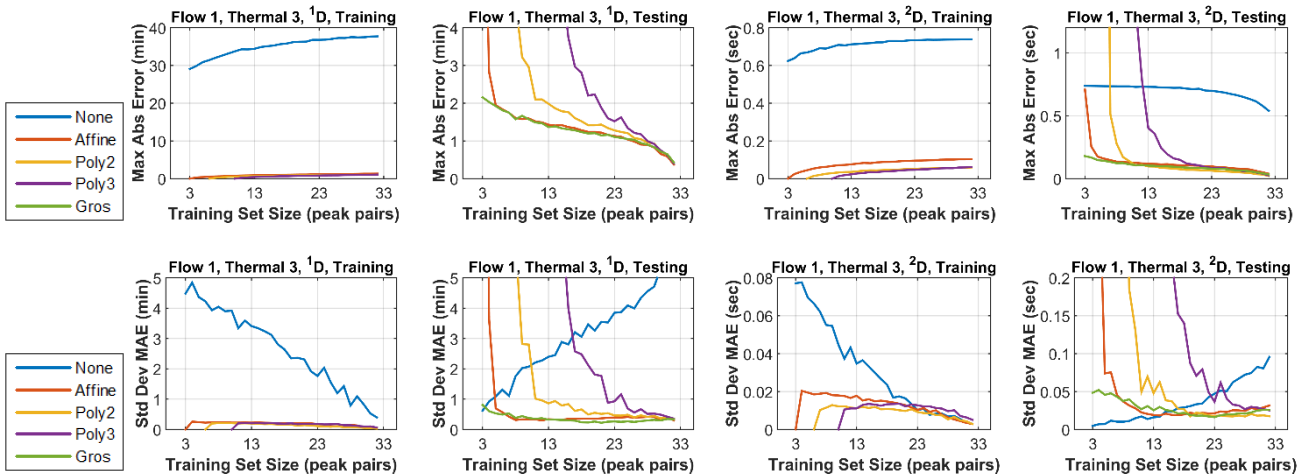
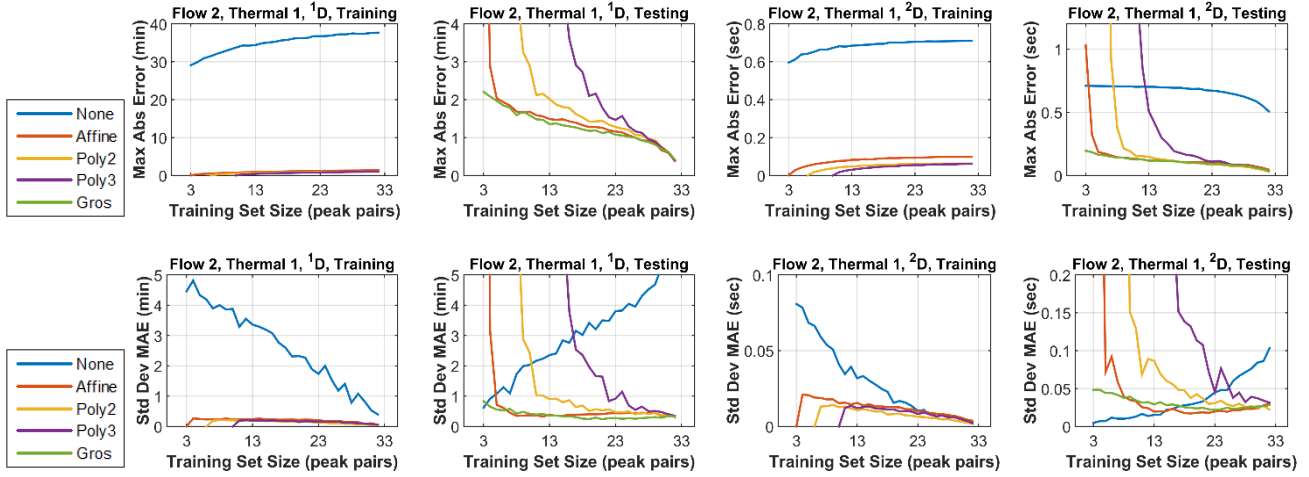
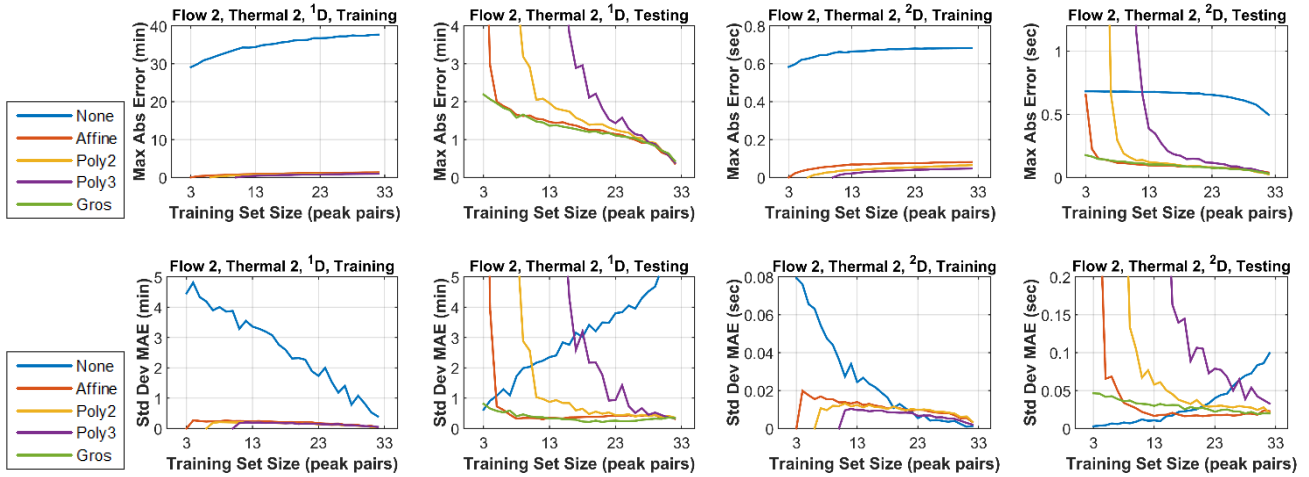


Figure S10. Maximum absolute error as a function of the training set size for alignment of GCxGC cocoa sample chromatograms with different modulation platforms. Columns from left to right are for ^1D with the training set, for ^1D with the testing set, for ^2D with the training set, and for ^2D with the testing set. Sets of rows with maximum absolute error on the top row of each set and the standard deviation of maximum absolute error on the bottom row of each set are for: A. Runs #1 and #1, B. Runs #1 and #2, C. Runs #1 and #3, D. Runs #2 and #1, E. Runs #2 and #2, and D. Runs #2 and #3.

D. Runs #2 and #1.



E. Runs #2 and #2.



F. Runs #2 and #3.

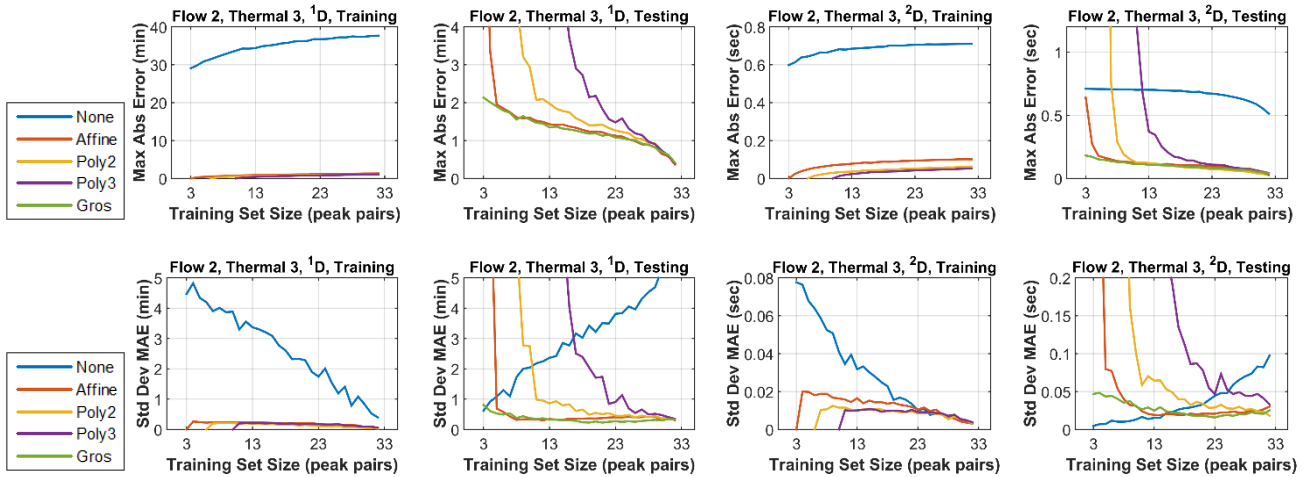


Figure S10 continued.

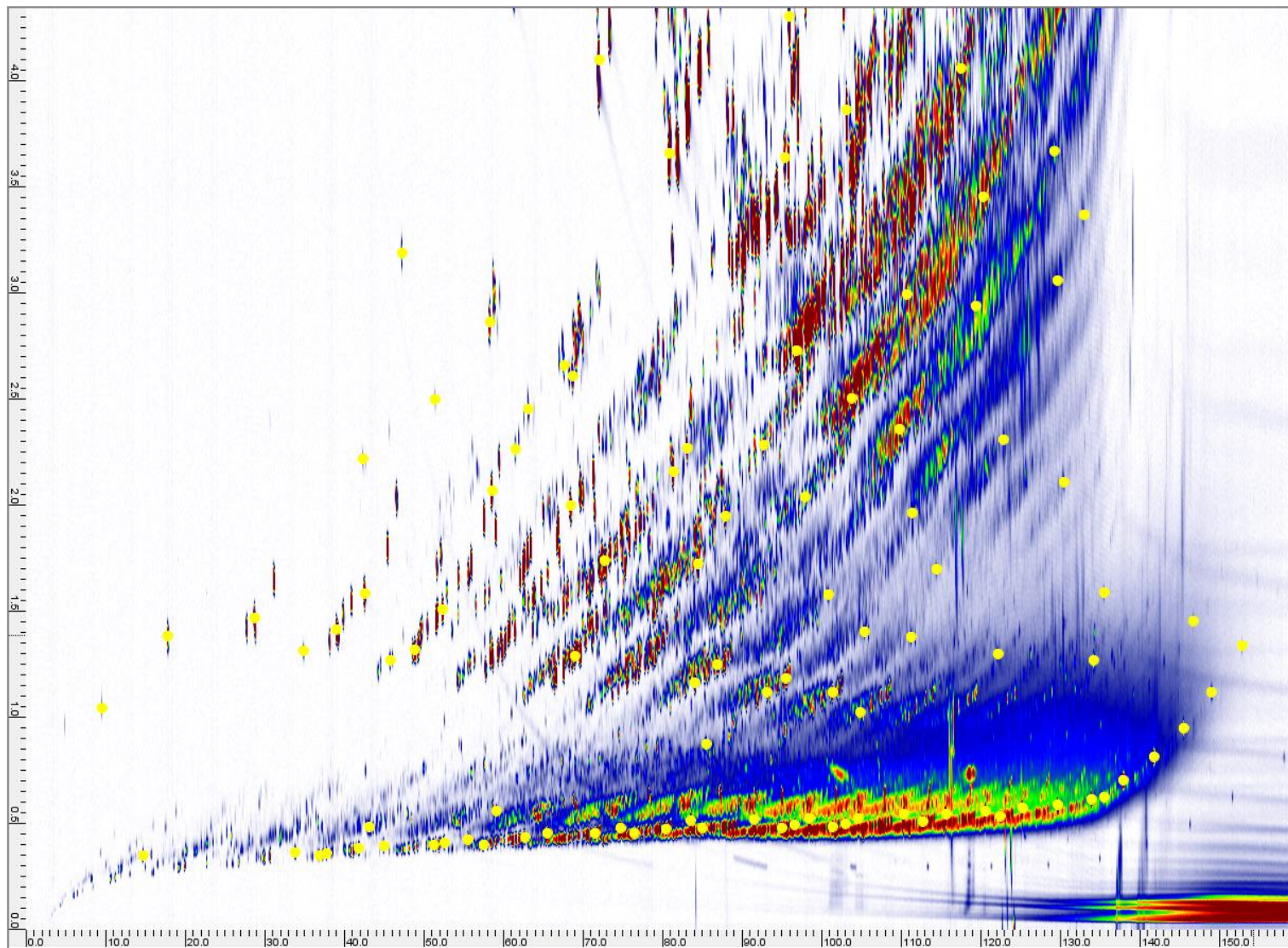


Figure S11. Diesel chromatogram 061413. Closed yellow circles represent peaks that were matched across all diesel chromatograms (112 peaks) and used as alignment points.

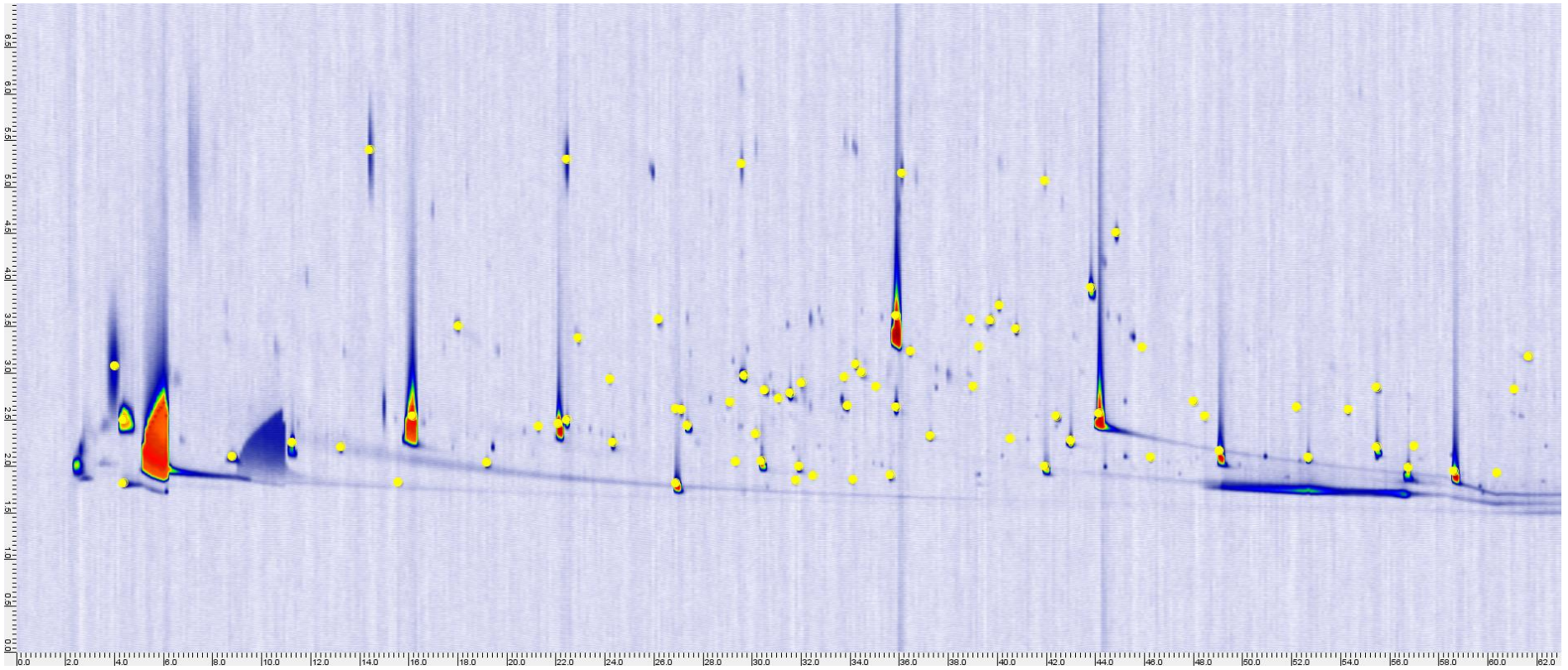


Figure S12. Wine chromatogram MC2011R2. Closed yellow circles represent peaks that were matched across all wine chromatograms (78 peaks) and used as alignment points.

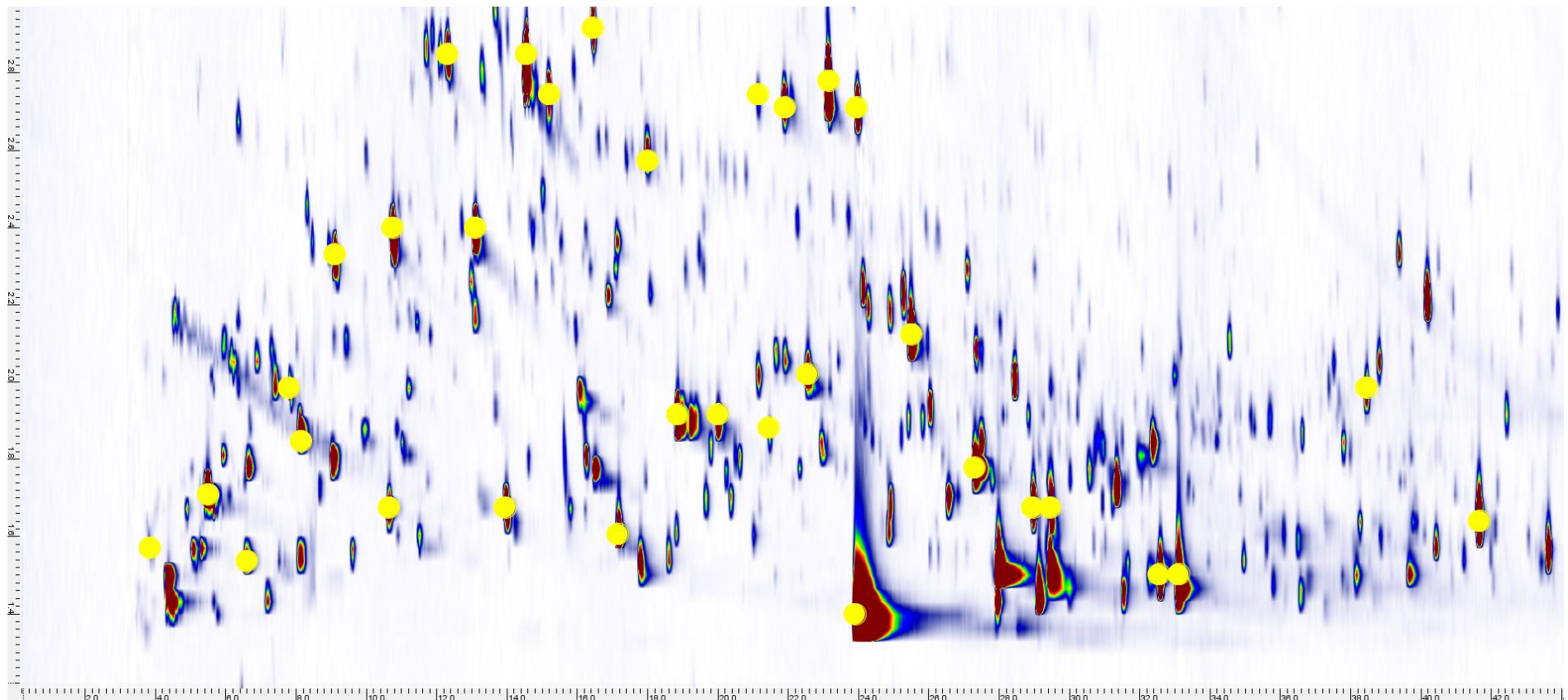


Figure S13. Cocoa sample chromatogram Thermal 1. Closed yellow circles represent peaks that were matched across all cocoa chromatograms (33 peaks) and used as alignment points.

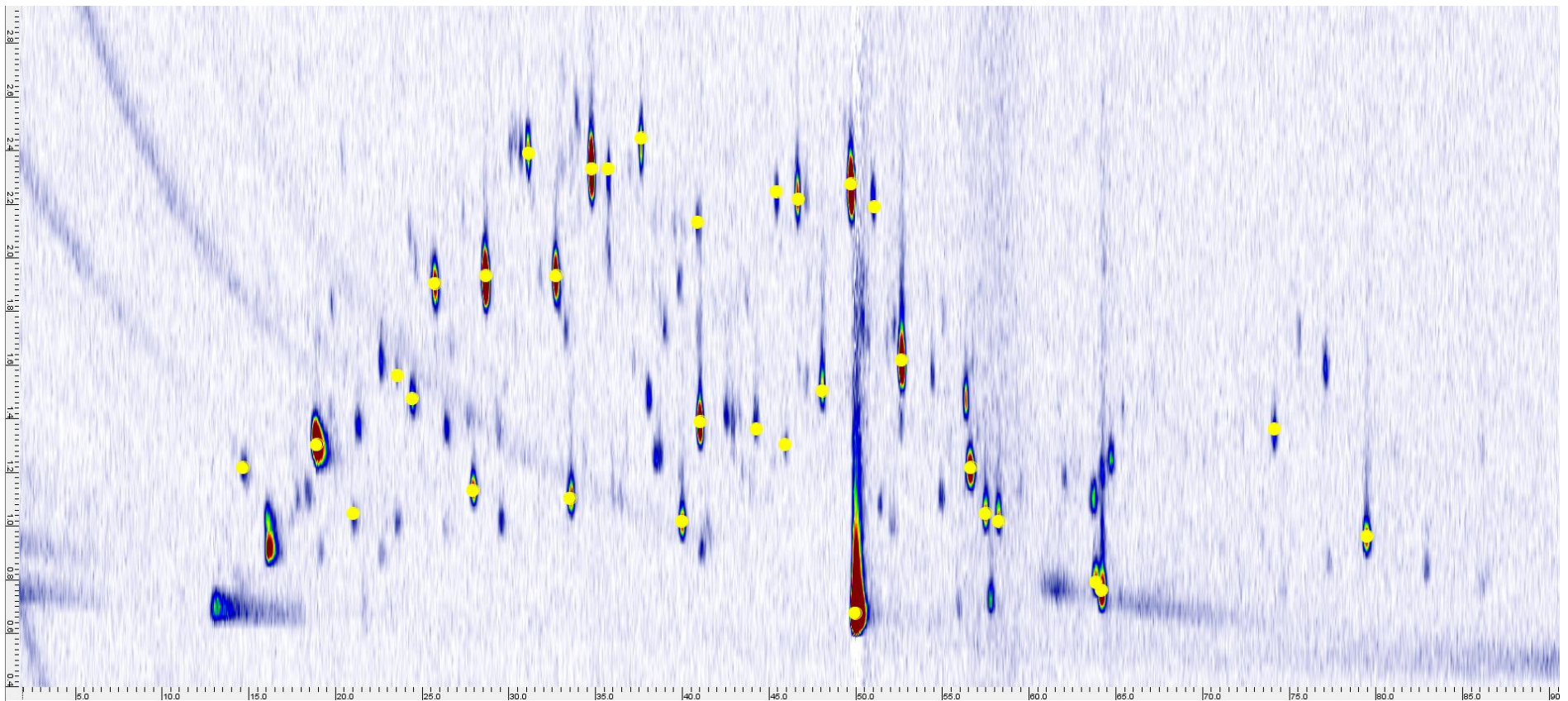


Figure S14. Cocoa sample chromatogram Flow 1. Closed yellow circles represent peaks that were matched across all cocoa chromatograms (33 peaks) and used as alignment points.